Electrical Power and Energy Systems 54 (2014) 352–366

Contents lists available at ScienceDirect

Electrical Power and Energy Systems

journal homepage: www.elsevier.com/locate/ijepes

Hierarchical management and control based on MAS for distribution grid via intelligent mode switching

Chun-xia Dou [a,*], Bin Liu [b,c]

[a] Institute of Electrical Engineering, Yanshan University, Qinhuangdao, 066004 Hebei, PR China
[b] School of Electrical & Information Engineering, The University of Sydney, NSW 2006, Australia
[c] Department of Information and Computation Sciences, Hunan University of Technology, Zhuzhou 412008, PR China

ARTICLE INFO

Article history:
Received 2 January 2013
Received in revised form 3 July 2013
Accepted 23 July 2013

Keywords:
Distribution grid
Multi-agent system
Hybrid control
Distributed energy resource
High-penetrated

ABSTRACT

Due to an increased penetration of distributed energy resources, as well as more uncertain operating environment, etc., present distribution power system is facing many challenges. For improving the performance regarding dynamic stability, self-healing, security, as well as economical and environmental benefit, this paper proposes a hierarchical management and control strategy for the high-penetrated distribution grid based on multi-agent systems structure via intelligent switching of operating mode. Corresponding to the complex hybrid behaviors, the hierarchical control scheme is designed as a three-level decentralized coordinated hybrid control. The simulation studies certify that the hierarchical hybrid control is effective and feasible to deal with comprehensive problems of high-penetrated distribution grids.

1. Introduction

With the interconnection of regional electric networks and the increased penetration of Distributed Energy Resources (DERs), present power systems are becoming more and more complex, and have been high-penetrated grids. Due to the developments of information and communication technology, advanced metering infrastructures and various power electronic control devices, power industries need rethink automation technique so that the high-penetrated grids can intelligently manage and control distributed energy resources to improve operation cost, reliability and power quality, etc.

However, compared with traditional power systems, the management and control for the high-penetrated grids is facing following new challenges:

1. *Containing large number of DERs.* A traditional power system only contains 50/60-Hz synchronous machines. But in a present high-penetrated grid, besides synchronous generators, there exist various DERs with different characteristics. Examples include variable frequency sources like wind energy sources, high frequency sources like micro-turbines, and direct energy conversion sources like fuel cells and photovoltaic sources [1,2]. The high penetration of DERs may impact on the reliability and the power quality of whole system, if these DERs cannot be effectively managed and controlled. However, the difference of dynamic behaviors of DERs will bring about more challenges to manage and control the grid.
2. *Displaying more frequent and more complex hybrid behaviors.* Under large disturbances, a high-penetrated grid usually shows complex hybrid dynamics behaviors including both continuous dynamic and event-driven behaviors [3]. Components such as synchronous machines, DER units and loads usually drive the continuous dynamic behavior complying with physical laws of dynamic characteristics, which may be represented as coupled differential equations and algebraic equations. Moreover, these components also exhibit event-driven discrete behaviors sometimes. Such as, the operating mode switching of DERS and the "plug-and-play" of DERs, these are event-driven discrete behaviors. Moreover, these discrete behaviors highly depend on and strongly impact on the continuous dynamic behaviors. Compared with traditional power systems, the high-penetrated grids usually appear more complex hybrid dynamic behaviors.
3. *Operating in a variable and uncertain environment.* In a high-penetrated grid, some renewable energy source units are subjected to natural conditions, such as wind energy sources and photovoltaic sources. Variable natural conditions result in the energy supply of these units uncertain and intermittent. In addition, there also are some distributed generation units to operate in the manner of "plug-and-play". That is to say, they may connect into network or disconnect form network at any time by some control commands. This "plug-and-play" also leads to the uncertainty of operating mode.

* Corresponding author. Tel.: +86 3358387556; fax: +86 3358072979.
E-mail addresses: cxdou@ysu.edu.cn (C.-x. Dou), bin.liu@sydney.edu.au (B. Liu).

0142-0615/$ - see front matter © 2013 Elsevier Ltd. All rights reserved.
http://dx.doi.org/10.1016/j.ijepes.2013.07.029

With respect to these new challenges, it is necessary to rethink management and control strategies for the present grids by using advanced new technologies.

Firstly, the management and control for the high-penetrated grids should be constructed as Multi-Agent System (MAS) based hierarchical control.

In the traditional power systems, energy management is ensured by a central energy management system in which a program is implemented. This program is based on some long series of power flow like "if else if" (e.g. "if the battery is empty then charge it"). Even if this solution achieves a constant supply of the load, it cannot fulfill easily other objectives such as fault tolerance of a unit. This centralized management requires the designer to be exhaustive in the power flow written in the program. If the configuration has to be changed (addition or removal of a unit) the program must be completely redesigned [4,5]. In addition, in the traditional grids, with respect to significant disturbance problems, "fit & forget" criterion is usually used to select controllable devices (e.g. "when a disturbance occurs, fit controllable devices are chose, other are forgot"), which implemented via a rule table [6,7]. This methodology highly depends on redundancy of controllable devices and requires the designer to be exhaustive in the predictable events written in the rule table. If an unpredictable event occurs it is unable to respond adequately. Moreover, if the configuration is changed, the rule table must be completely redesigned too. Therefore, traditional power systems lack flexibility and adaptability to uncertain operation situation.

Taking account into the complexity of present grids and the diversity of DERs, in order to improve the performance regarding security and reliability, the management and control for high-penetrated grids should be constructed as MAS based hierarchical control. MAS is composed of multiple agents, which depend on each other in cooperation and competition environment to form a community to achieve the goals of individuals and the whole system [8,9]. And the MAS based control is able to offer following desirable properties to overcome the new challenges of present grids [10,11].

1. *The feasibility of control for complex system*; with respect to the MAS based hierarchical control, the dynamic performance of each DER unit is regulated by unit agent, the controllable devices are managed by discrete coordinated control agent, and the energy management is ensured by a central agent. The different hierarchical agents can achieve respective goal mostly autonomously. And they can also work in parallel in a cooperative environment to achieve the goals of system. Differed from the traditional central energy management, in the MAS based hierarchical control, in the face of unpredictable events, each unit can respond separately and the constraints of each unit can be adequately handled by the agent itself, and the requirement of ability in computation and communication for the central energy management is largely decreased. Therefore, w.r.t. the high-penetrated grid, the control scheme is feasible and efficient.
2. *The adaptability to uncertain environment*; with respect to the MAS based hierarchical control, the different hierarchical agents can respond quickly to the emergencies of environment by respective reactive layer. And they also have high intelligence to control or plan the behaviors of agent so as to achieve their desires or intentions by respective deliberative layer. Moreover, through their interactions, the different hierarchical agents can depend on each other to adjust their operating state according to the variable and uncertain environment.
3. *Reliability of control*; with respect to the MAS based hierarchical control, in case one or more agents fail, other agents may maintain the system normal operation. Because the different hierarchical agents work in decentralized and coordinated manner, the fault of one or more agents cannot make the overall system useless.
4. *Reduced data manipulation*; with respect to the MAS based hierarchical control, the local dynamic information should be firstly processed within respective agent, and the information exchanged among agents should be knowledge information. In this way, the amount of information exchanged is largely decreased.
5. *Intelligent switching of operating mode*; with respect to the MAS based hierarchical control, through the interactions among the different hierarchical agents, the operating mode of generation or load units can be coordinately switched according to the change of the operating condition.

For the above reasons, the MAS based control may be an interesting candidate in order to control DERs in a flexible manner so that the high-penetrated distribution grid can meet the variable energy demand with high reliability, flexibility and effective cost even in uncertain operation situation. So in this paper, the MAS based hierarchical control is proposed to develop the management and control for present high-penetrated distribution grids.

In addition, corresponding to the complex hybrid behaviors, the management and control for the high-penetrated grids should be reconstructed as hybrid control.

In traditional power systems, due to the imperfectness in information and communication technology, there is less interaction between discrete event management and continuous dynamic control. This leads to the automation level of whole system in a lower degree [12,13]. With developments of information and communication technology, the automatic control for present high-penetrated grids should be reconstructed as hybrid control. That is to say, the present high-penetrated grids not only require continuous controller to regulate the dynamic behaviors, but also need discrete control commands to manage event-driven discrete behaviors, and it is the most needful that there are real-time interactions between discrete event management and continuous dynamic control. That is just the idea of hybrid control.

Recently, hybrid control theory has attracted much attention in complex system areas. It is the evolution of multi-mode control with some specific characteristics that provide new capabilities in controlling complex hybrid systems. As an effective means, the control technology has already been proposed in power system, and a few contributions have been made. In [14], after describing various power system events, the hybrid dynamic behavior between discrete controllable events and dynamic system is analyzed based on hybrid model. In [15], modeling and switching stability analysis of hybrid power system with on-load tap changer (OLTC) are researched. For the purpose of enhancing overall stability performance, a global hybrid control involving coordination of many controls with diverse goals was developed in [12]. A global control scheme using an ultra-capacitor fuel cell (UPFC) combined with generator excitation control, PSS and capacitor switching, was proposed to implement coordinated control over all three major dynamic issues in [13]. In [16], a hybrid system is found by using two cascaded regulators. And in [17], Authors firstly proposed a two level hybrid control for wide-area power systems based on hybrid system theory. On the basis of [17], in [18], a herarchical hybrid control is presented by authors for improving comprehensive performance in smart power system.

In this paper, on the basis of the previous researches, for improving the performance regarding dynamic stability, self-healing, security, as well as economical and environmental benefit, MAS based hierarchical hybrid control is developed for the high-penetrated distribution grids.

The research is decomposed in several stages, starting with designing the structure of MAS based hierarchical hybrid control, which consists of one upper level energy management agent, several middle level discrete coordinated control agents and many lower level unit control agents.

On the next stage, the upper level energy management agent is studied. This agent is mainly responsible for energy assignment for the purpose of maximum economic and environmental benefits. In this agent, the energy management models is built based on Colored Petri-Net (CPN), and the energy management strategies are drafted by using multi-objective optimization method.

On the third stage, the middle level discrete coordinated control agents are designed. The middle level agents are mainly responsible for switching the operating modes of the lower level unit agents by discrete coordinated control commands for the purpose of self-healing and security at emergencies. The operating mode collaboration models is built based on G-Nets, and the discrete control commands are drafted based on the stability risk indexes regarding voltages and frequency.

On the final stage, the design of the lower level unit control agents is presented in the general form. Their main functions are to control local loads, DER units, synchronous generator units and discrete component units, etc. according to commands from the senior level agents so as to obtain satisfactory stabilization performance.

2. The structure of MAS based hierarchical hybrid control

In this paper, let us take a 10-kV distribution system connected to the main grid as an example of high-penetrated distribution grid as shown in Fig. 1, where the main grid is represented as a capacity bus. The distribution system is divided into two regions according to the degree of electrical coupling, and each region respectively includes a generator unit, a storage unit, a renewable units and a load unit. With respect to the distribution system, the MAS based hierarchical control is constructed, where there are one upper level energy management agent for whole system, two middle level regional coordinated control agents and eight unit agents designed. A combination of non-sensitive load units 1, 2 and 6, and sensitive loads units 3, 4, 5, 7 and 8 is supplied through two radial feeders of the system. The architecture of every agent is designed as shown in Fig. 2, which is composed of both reactive and deliberative layer. The reactive layer that is defined as "recognition, perception and action" has priority to respond quickly to emergencies of environment. Such as, the reactive layer of wind energy generation unit agent can perceive the sudden change of wind speed so as to determine whether it should act immediately to ask for switching operation mode. And the deliberative layer that is defined as "belief, desire and intention" has high intelligence to control or plan the behaviors of agent so as to achieve its desire or intention.

And the block diagram of the MAS based hierarchical hybrid control is shown as Fig. 3. With respect to the hierarchical MAS, the control goal of each generation or load unit is carried out by their respective unit agents. The coordinated control for operation modes is implemented through the middle level agent by region. The energy optimization problem of whole system is deal with by an upper level agent. The detailed explanation is given as follows.

The upper level energy management agent is composed of multi-function modules, such as communication module, knowledge base module, data collection module, decision making module and action implementation module, by which the goal of energy optimization assignment is achieved. Firstly, the dynamic information regarding the network and the operating states of the system are collected in the data collection module via its acquisition, monitor and learning functions. By using the collected information integrated with the knowledge data, the energy management strategies are determined in the decision making module, which will be discussed in Section 3. And the energy assignment strategies are implemented via the action implementation module. In whole system, there is only one energy management agent to handle the energy optimization problem of whole grid.

The coordinated control of operating mode is the goal of the middle level agents, which is also achieved by multi-function modules including communication module, data collection module, decision making module and action implementation module. The coordinated switching control is drafted in decision making module by using the state information from the data collection module, which will be discussed in Section 4. The switching control is implemented via the action implementation module. In each local region, there is only one middle level agent to control the operating modes of all lower level unit agents that reside in this region.

The goal of the lower level unit control agents is to manage the dynamic performance of respective component unit. For instance, the energy source agent can decide what time to connect/disconnect its generation unit into/from the network by some control commands, as well regulate the dynamic performance of its generation unit based on the local states and the interaction with other agents. The main module of the unit agent is continuous controller, which is designed in a decentralized manner based on local state information. Because of the difference of dynamic characteristics, the design of their continuous controllers is also very different issue.

In the MAS based hierarchical control, the interactions among agents include both direct and indirect interactions. From top to bottom, the energy assignment from the upper level agent to the group of unit agents, and the coordinated control for operation mode from the middle level agent to the group of unit agents, are direct interactions through control command transmissions, which will be discussed in Sections 3.1 and 4.1 respectively. Conversely, the interactions form the lower level agents to the both upper level and middle level agents are indirect interactions based on the communication transmissions.

3. The upper level energy management agent

The most key components of the upper level agent are the decision making module that is responsible for determining the energy management strategies and the action implement module that is responsible for implementing energy assignment. Therefore, in this section, the researches are focused on how to establish the energy management strategies and how to implement the energy assignment through interactive behaviors based on an energy management model.

3.1. The energy management model

In order to carry out the energy assignment, the energy management cooperation model from the upper level agent to the lower level unit agents is designed by using CPN as shown in Fig. 4.

A CPN can be defined by a 9-tuple (Σ, P, T, A, N, C, G, E, I), where Σ is a set of nonempty types, also called colored sets; P is a set of places; T is a set of transitions; A is a set of arcs. N is a node function; C is color function; G is a guard function; E is an arc expression function; and I is an initialization function [19].

The CPN differs from Petri Net (PN), because their tokens are not simply markers, but are colored markers associated with data. The places of CPN may contain multiple sets of tokens. The arcs of CPN can carry out or specify some transfer conditions. All arcs have an associated constrain function to determine which elements to be

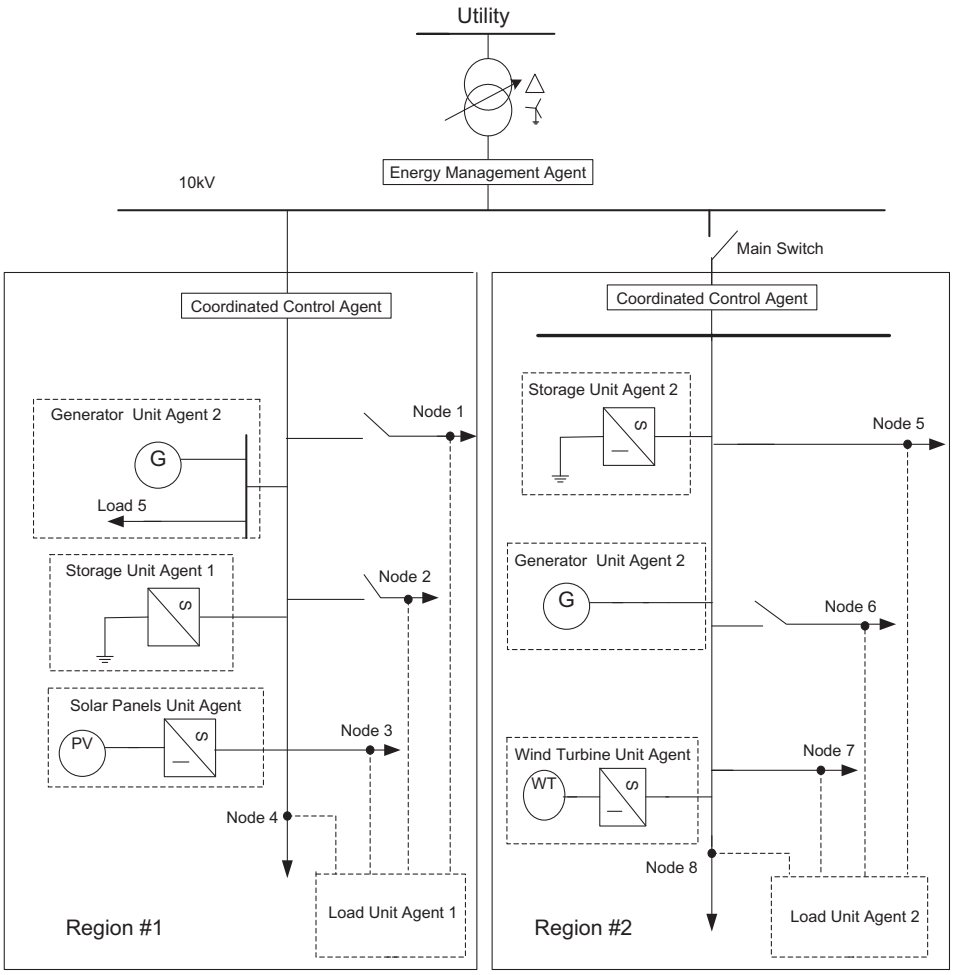

Fig. 1. The diagram of high-penetrated distribution grid.

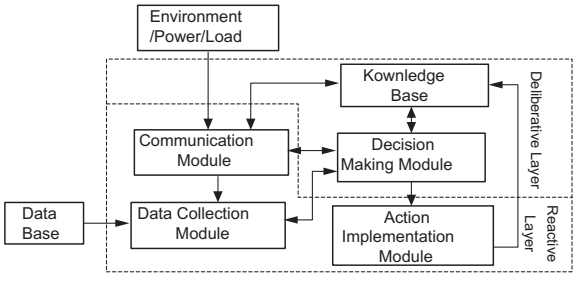

Fig. 2. Architecture of every agent.

removed or hold. Transitions of CPN are associated with some guard functions that enforce some constraints on tokens. Just because of these features, the CPN is selected to describe the interactions between the upper level agent and the lower level unit agents.

In the CPN as shown in Fig. 4, PS = $\{PS_1, PS_2, \ldots, PS_n\}$ represents power prediction token, and $PS_1, PS_2, \ldots, PS_n$ denote power production projects of generation $unit_1, unit_2, \ldots, unit_n$ respectively. $\langle ps_1\rangle, \langle ps_2\rangle, \ldots, \langle ps_n\rangle$ are elements of $PS_1, PS_2, \ldots, PS_n$ respectively, which are acquired by power prediction of electricity plants. Similarly, UD = $\{UD_1, UD_2, \ldots, UD_m\}$ represents load forecast token, and $UD_1, UD_2, \ldots, UD_m$ denote energy demands of load $unit_1$, $unit_2, \ldots, unit_m$ respectively. $\langle ud_1\rangle, \langle ud_2\rangle, \ldots, \langle ud_m\rangle$ are elements of $UD_1, UD_2, \ldots, UD_m$ respectively, which are acquired by load forecasting from users. $\langle ps_1, ud_1\rangle, \langle ps_1, ud_2\rangle, \ldots, \langle ps_1, ud_m\rangle$ represent the power assignment that the generation $unit_1$ supplies to the load $unit_1, unit_2, \ldots, unit_m$ respectively. Similarly, $\langle ps_n, ud_1\rangle, \langle ps_n, ud_2\rangle, \ldots, \langle ps_n, ud_m\rangle$ denote the assignment that the generation $unit_n$ provides to the load $unit_1, unit_2, \ldots, unit_m$ respectively, which are determined by optimization energy management strategies. Then, all lower level generation units will regulate their power outputs and all lower level load units will also control their demands according to the power assignment plan.

In Fig. 3, all places (P), all transitions (T) and all arcs (A) have been shown. Besides, D = {PS, UD}, E− and E+ functions are determined by the energy management strategies. The initial marking: m0(p1—power prediction) = {PS}, m0(p2—user forecasting) = {UD}, m0(other places) = null.

And the successor token

$$M'(P) = M(P) - E_-(P,T) + E_+(T,P).$$

3.2. The energy management strategies

3.2.1. The multiple objective optimization functions

(1) The objective function regarding economical index is constructed as follows

$$O_1 = \min\left\{\sum_{i=1}^{n_d}\phi_{is}[(h_{iD} * F_{isD}(P_{isD}) + M_{iD}(P_{isD}) + \lambda_{isD}C_{stiD}] + \sum_{j=1}^{n_g}[(h_{jG} * F_{jG}(P_{jG}) + M_{jG}(P_{jG})]\right\}, \quad (1)$$

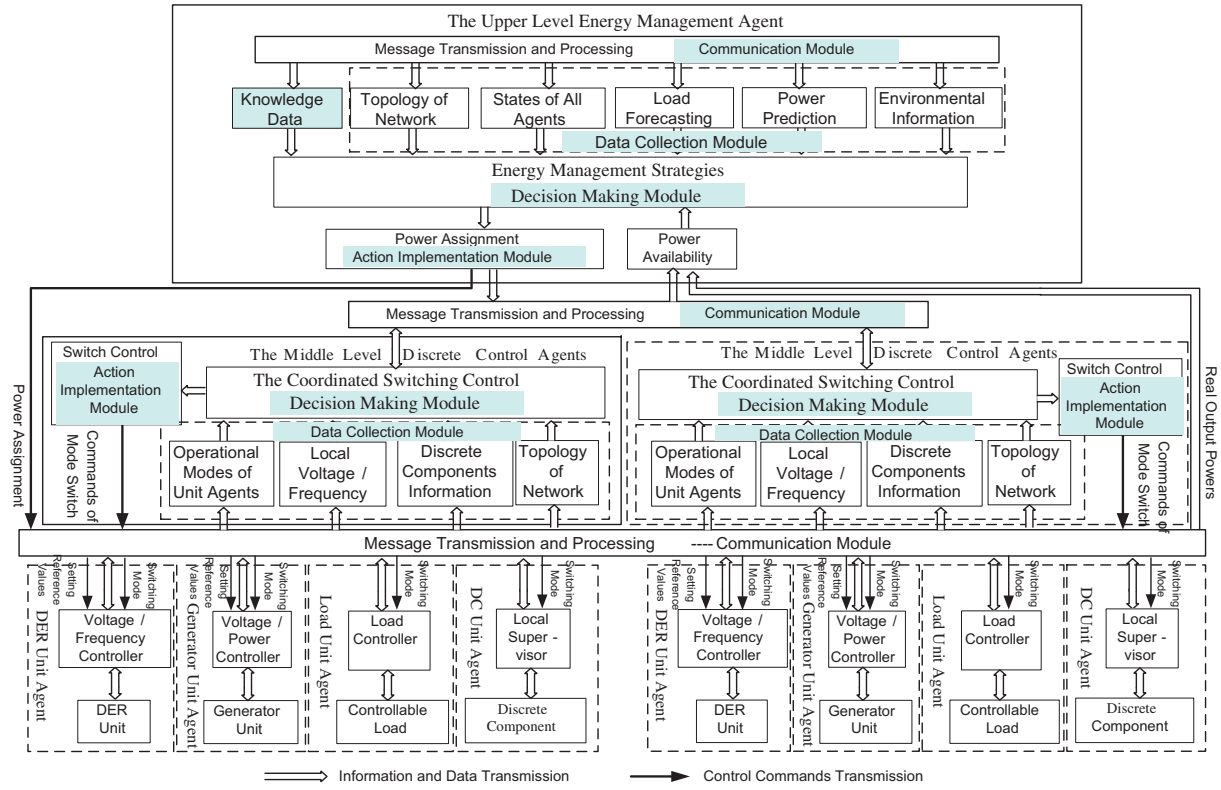

Fig. 3. The block diagram of the MAS based hierarchical hybrid control.

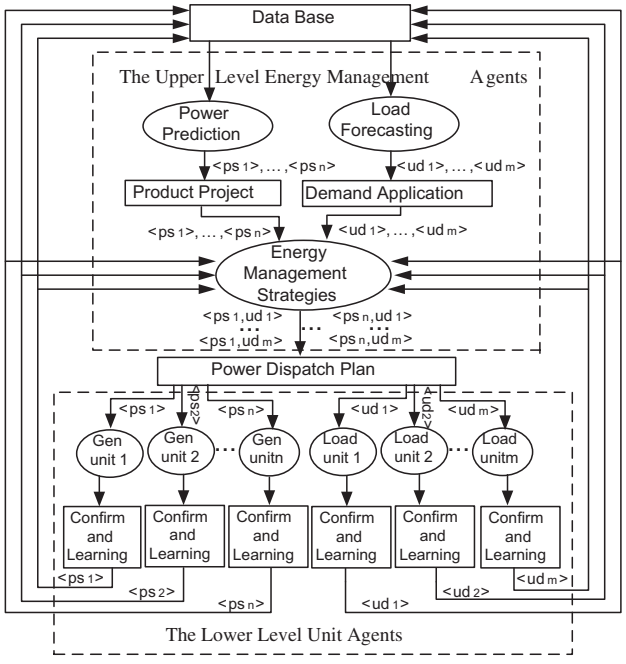

Fig. 4. The energy management models from the upper level agent to the lower level unit agents.

where $i \in \{1,2,\ldots,n_d\}$, and n_d is the number of DERs in grid. $s \in \{1,2,\ldots,S_i\}$ represent the operating mode of ith DER unit. $F_{isD}(P_{isD})$ denotes the consumption characteristic function of ith DER on sth operating mode. h_{iD} is the unit fuel price of ith DER. versus renewable energy resources, $h_i \equiv 0$. $M_{iD}(P_{isD})$ represents maintenance cost of ith DER. C_{stiD} is the starting cost of ith DER, $\lambda_{isD} \in \{0,1\}$, when the ith DER is in starting state, $\lambda_{isD} = 1$, otherwise, $\lambda_{isD} = 0$. $\phi_{is} \in [0,1]$, versus the operating mode, $\phi_{is} = 1$, and versus stopping mode, $\phi_{is} = 0$. $j \in \{1,2,\ldots,n_g\}$, and n_g is the number of traditional generators in grid. $F_{jG}(P_{jG})$ denotes the consumption characteristic function of jth generator. h_{jG} is the unit fuel price of jth generator. $M_{jG}(P_{jG})$ represents maintenance cost of jth generator, which is deemed in proportion to P_{jG} and described as $M_{jG}(P_{jG}) = K_j P_{jG}$, K_j is coefficient.

For traditional generators, the consumption characteristic function is described as

$$F_{jG}(P_{jG}) = c_{0j} + c_{1j}P_{jG} + c_{2j}P_{jG}^2, \tag{2}$$

where c_{0j},c_{1j} and c_{2j} are coefficients.

And for other DERs such as fuel cell and micro-turbine, the consumption characteristic function is described as

$$F_{isD}(P_{isD}) = D_{is}P_{isD}/\eta(P_{isD}), \tag{3}$$

where D_{is} is coefficient. $\eta(P_{isD})$ is operating efficiency.

(2) The objective function regarding pollution emission index is constructed as follows

$$O_2 = \min\left\{\sum_{i=1}^{n_d}\sum_{k=1}^{P}\phi_{is}g_{isd}^k P_{isD} + \sum_{j=1}^{n_g}\sum_{l=1}^{Q}g_{jg}^l P_{jG}\right\}, \tag{4}$$

where $k \in \{1,2,\ldots,P\}$, and P is the kind number of emission substances in DER. g_{isd}^k represents the punishment fee of unit power for kth kind emission in ith DER on sth operating mode. versus renewable energy resources, $g_{is}^k \equiv 0$. Similarly, $l \in \{1,2,\ldots,Q\}$, and Q is the kind number of emission substances in generator. g_{jg}^l represents the punishment fee of unit power for lth kind emission in jth generator.

3.2.2. Constraint conditions

(1) The constraint conditions of generating electricity

$$P_{isD\min} \leqslant P_{isD} \leqslant P_{isD\max}; \tag{5}$$

$$P_{jG\min} \leqslant P_{jG} \leqslant P_{jG\max}.. \tag{6}$$

(2) The constraint conditions of storage energies

$$P_{sE,di,\min} \leqslant P_{sE,di} \leqslant P_{sE,di,\max}; \tag{7}$$

$$P_{sE,ci,\min} \leqslant P_{sE,ci} \leqslant P_{sE,ci,\max}; \tag{8}$$

$$E_{sE,i,\min} \leqslant E_{sE,i} \leqslant E_{sE,i,\max}; \tag{9}$$

where $i \in \{1,2,\ldots,n_e\}$, and n_e is the number of storage energy units. $P_{sE,di}$ and $P_{sE,ci}$ are discharge and charge powers respectively, and $E_{sE,i}$ is the capacity of ith storage energy unit.

(3) The constraint conditions of whole system

$$\sum_{i=1}^{n_d} P_{isD} + \sum_{j=1}^{n_g} P_{jG} + \sum_{i=1}^{n_e} [P_{sE.di} - P_{sE,ci}] - \sum_{i=1}^{m} P_{loadi} = 0, \tag{10}$$

where P_{loadi} is the demand power of ith load unit agent. When a storage energy unit operates in discharge mode, $P_{sE,ci} = 0$; otherwise, in charge mode, $P_{sE,di} = 0$.

3.2.3. Multi-objective function optimization

The multi-objective optimization function is constructed as

$$O = \min\left\{[\gamma_1 O_1 + \gamma_2 O_2] + \sigma\left(\sum_{i=1}^{n_d} P_{isD} + \sum_{j=1}^{n_g} P_{jG} + \sum_{i=1}^{n_e} [P_{sE.di} - P_{sE,ci}] - \sum_{i=1}^{m} P_{loadi}\right)\right\}, \tag{11}$$

where γ_1 and γ_2 are the weight coefficients of each objective function respectively. σ is punishment factor.

The energy management strategies of the upper level agent can be drafted based on (11) by using multi-objective optimization methods in [20].

4. The middle level discrete coordinated control agents

In this section, the researches are focused on how to establish the discrete coordinated control commands and how to implement operating mode switch through interactive behaviors based on an operating mode cooperation control model.

4.1. The operating mode cooperation control model

The operating mode cooperation models from the middle level agent to the lower level unit agents are designed by using an agent-based G-net mode as shown in Fig. 5. The G-net is an agent-based Petri-net that is defined by a 5-tuple AG = (GSP, GL, KB, PL, IS), where GSP is a generic place providing an abstract for the agent-based G-net; GL is a goal module; KB is a knowledge-base module; PL is a planner module and IS is an internal structure of AG [21].

In this paper, the middle level agent is responsible for coordinately switching the operation mode of all lower level unit agents in its region. Thus, it need know an abstract regarding the operation mode of all unit agents and provide a control goal, then based on knowledge data, constitutes the coordinated control strategies for all unit agents. The agent-based G-net is very suitable to design the interactions between the middle level agent and the lower level unit agents, because it possesses the above corresponding functions. Detailed design are given as follows.

GSP is designed as to describe the abstract regarding the operating modes of all unit agents; GL provide control goals of voltage or frequency; PL is designed as the coordinated control strategies including interfaces and coordinated control commands, which has the functions of dispatching messages, determining the next operating mode, starting a new switching; IS is composed by the lower level unit agent group, which is described by using Petri-net model. In following sections, researches are focus on the design of IS regarding unit agent group and PL of middle level agent.

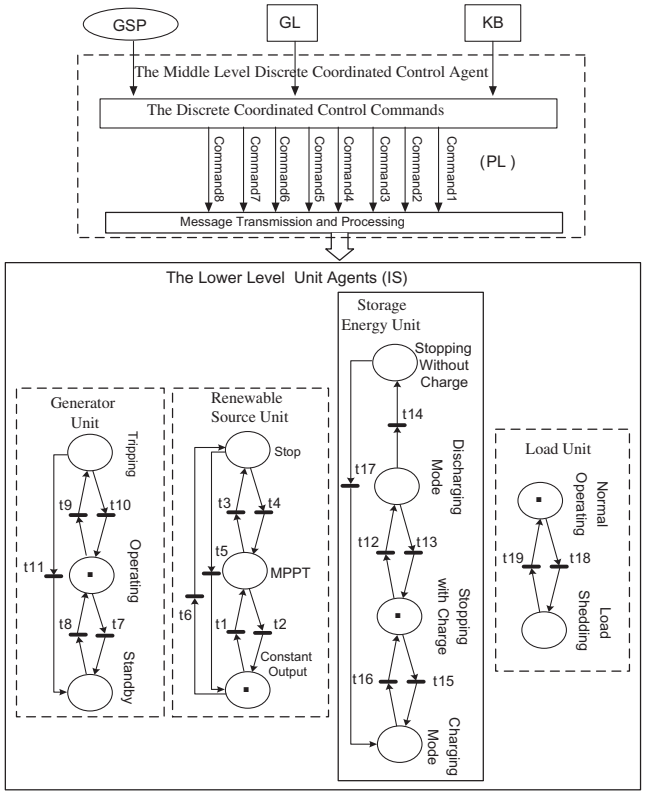

Fig. 5. The operating mode coordination control models from the middle level agent to the lower level unit agents.

4.2. Design of internal structures regarding unit agent group based on PN

The operation of renewable energy generating unit strongly depends on natural energy conditions. In order to maximize economical benefit, such unit ordinarily runs in Maximum Power Point Tracking (MPPT) mode. Only when the voltage is higher than the maximum safe voltage of 1.05, the unit must be switched into constant output mode. When natural energy drops to a less value, such unit will have to stop operating. The operating mode of renewable

Table 1
Descriptions of transitions in renewable energy unit agent.

Transitions	Description
t1	The voltage drops to less than the maximum safe voltage of 1.05
t2	The voltages rise to larger than the maximum safe voltage of 1.05
t3	The natural energy decreases to less than minimum allowable value so that the unit has to stop operation
t4	The natural energy increases to larger than minimum allowable value so that the unit starts to operate
t5	When this unit is in stopping state, the middle level agent sends control command to request starting so as to increase constant power output
t6	When this unit is in constant output state, the middle level agent sends control command to request stopping so as to decrease power output

Table 2
Descriptions of transitions in generator unit agent.

Transitions	Description
t7	When this unit is in rated state, the middle level agent sends control command to request stopping so as to decrease power output
t8	The middle level agent sends control command to request restarting and returning to rated state
t9	A fault lead to the generator tripping
t10	The line is restored so that the generator unit returns to rated state
t11	The generator in tripping state is ready to operate

Table 3
Descriptions of transitions in storage energy unit agent.

Transitions	Description
t12	When this unit is in stopping state with charge, the middle level agent sends control command to request discharging so as to increase power output
t13	The middle level agent sends control command to request stopping discharge so as to decrease power output
t14	The storage energy unit discharges to minimum allowable value of State of Charge (SOC)
t15	When this unit is in stop state with charge, the middle level agent sends control command to request charging so as to decrease power output
t16	The storage energy unit charges to maximum allowable value of SOC
t17	The storage energy unit requests charging

Table 4
Descriptions of transitions in load unit agent.

Transitions	Description
t18	When this unit is in normal state, the middle level agent sends control command to request load shedding so as to decrease power demand
t19	The middle level agent sends control command to request restoring load

energy unit agent is described based on PN as shown in Fig. 4. And the descriptions of switch conditions called as transitions are given in Table 1.

The operating mode of generator unit agent is also shown in Fig. 4. And the descriptions of switch conditions are given in Table 2.

The energy storage unit agent is usually responsible for maintaining the balance between supply and demand by the frequent switching of operating mode. The operating mode of energy storage unit agent is also described based on PN. And the descriptions of transitions are given in Table 3.

The load unit agent is responsible for making its demand controllable according to coordinated control commands. The operating mode of load agent is also shown in Fig. 4. And the descriptions of transitions are given in Table 4.

4.3. Design of PL regarding the coordinated control of the middle level agent

In this section, the discrete coordinated control is determined based on characteristic parameters.

4.3.1. Characteristic parameters regarding stability

4.3.1.1. The characteristic parameters related to voltage stability. Because the voltage instability generally manifests itself, initially, as a slow decay of the voltage following a sharp decline at the point of collapse, so the dynamic voltage alone cannot be a reliable indicator of the voltage instability, and using a threshold value on the voltage to detect instability may lead to wrong conclusions. In this paper, a dynamic voltage stability criterion based on the Voltage Stability Risk Index (VSRI) is used to assess whether the system is able to achieve a post-disturbance stable state for voltages [22,23].

Let the PMU measurements for ith bus voltage be $V_i = \left[V_i^1, V_i^2, \ldots, V_i^m\right]^T$ at a rate of 30 frames/s in a 60 Hz system or 25 frames/s in a 50 Hz system, the VSRI is formulated as follows:

(1) The moving average value of the bus voltage at jth instant from N available PMU measurements

$$V_i^{(j)} = \sum_{k=1}^{j} V_i^k/j \quad j \in 1,2,\ldots,N; \quad \text{if } j \leqslant N; \tag{12}$$

$$V_i^{(j)} = \sum_{k=j-N+1}^{j} V_i^k/N \quad j \in N+1, N+2, \ldots, m; \quad \text{if } j > N. \tag{13}$$

(2) The percentage diversity between the voltage measured at jth instant V_i^j and the moving average value $V_i^{(j)}$

$$C_i^j = \frac{V_i^j - V_i^{(j)}}{V_i^{(j)}} \times 100, \quad (j \in 1,2,\ldots,m). \tag{14}$$

(3) The VSRI at jth instant by dividing the area under the percentage diversity curve by N

$$\mathrm{VSRI}_i^{(j)} = \sum_{k=1}^{j} \left(C_i^k + C_i^{k-1}\right)/2j \;\; j \in 1,2,\ldots,N; \;\; \text{if } j \leqslant N; \tag{15}$$

$$\mathrm{VSRI}_i^{(j)} = \sum_{k=j-N+1}^{j} \left(C_i^k + C_i^{k-1}\right)/2N, \;\; j \in N+1, N+2, \ldots, m; \;\; \text{if } j > N. \tag{16}$$

The following characteristics of the VSRI are used to develop a dynamic voltage stability criterion.

(i) The bus with the largest positive or smallest negative index at any given time has the highest risk of the voltage instability.
(ii) If the post-disturbance voltages are stable, the VSRIs at all buses converge to zero.

4.3.1.2. The characteristic parameters related to frequency stability. Frequency is unique in the whole system and it is enough to measure in one node in the system. In this paper, a dynamic frequency stability criterion based on the Frequency Stability Risk Index (FSRI) is used to assess whether the system is able to achieve a post-disturbance stable state for frequency. Let the PMU measurements be $f = [f_1, f_2, \ldots, f_m]^T$, the FSRI is formulated as follows:

(1) The moving average value at jth instant from N available PMU measurements

$$f^{(j)} = \sum_{k=1}^{j} f_k/j \quad j \in 1,2,\ldots,N; \quad \text{if } j \leqslant N; \tag{17}$$

$$f^{(j)} = \sum_{k=j-N+1}^{j} f_k/N \quad j \in N+1, N+2, \ldots, m; \quad \text{if } j > N. \tag{18}$$

(2) The percentage diversity between the frequency measured at jth instant f_j and the moving average value $f^{(j)}$

$$D^j = \frac{f_j - f^{(j)}}{f^{(j)}} \times 100, \quad (j \in 1,2,\ldots,m). \tag{19}$$

(3) The FSRI at jth instant by dividing the area under the percentage diversity curve by N

$$\mathrm{FSRI}^{(j)} = \sum_{k=1}^{j}(D^k + D^{k-1})/2j \quad j \in 1,2,\ldots,N; \quad \text{if } j \leqslant N; \tag{20}$$

$$\mathrm{FSRI}^{(j)} = \sum_{k=j-N+1}^{j}(D^k + D^{k-1})/2N, \quad j \in N+1, N+2,\ldots,m; \quad \text{if } j > N. \tag{21}$$

The following characteristics of the FSRI are used to develop a dynamic frequency stability criterion.

(i) The system with the largest positive or smallest negative index at any given time has the highest risk of the frequency instability;
(ii) If the post-disturbance frequency is stable, the FSRI of system converges to zero.

4.3.2. The logic control commands

Following a large disturbance, if at least a stability risk index (SRI) exceeds its alarming value, it implies that the system is unable to achieve post-disturbance stabilization. And the middle level coordinated control agent need be triggered so as to send corresponding control commands to lower level unit agents in order to switch their operating modes and rapidly stabilize the system down. The threshold values of these stability risk indexes can be enacted in critical working conditions in an offline manner by simulation software in advance. The threshold values of voltage and frequency are defined as $\varepsilon_{1,threshold}$ and $\varepsilon_{2,threshold}$ respectively. Then, according to whether the thresholds are violated, the conclusions regarding stability are drawn as follows:

Voltage instability, if $\left|\mathrm{VSRI}_i^{(j)}\right| \geqslant \varepsilon_{1,threshold}$.
Voltage stability, if $\left|\mathrm{VSRI}_i^{(j)}\right| < \varepsilon_{1,threshold}$.
Frequency instability, if $|\mathrm{FSRI}^{(j)}| \geqslant \varepsilon_{2,threshold}$.
Frequency stability, if $|\mathrm{FSRI}^{(j)}| < \varepsilon_{2,threshold}$.

In this research, except discrete components, such as relay and circuit breakers, often have control commands itself for switch on or off to isolate a fault by sensing line currents, other unit agents have switching control by the coordinated control of operating modes. For example, according to the FSRI, the switching control regarding frequency are drafted as follows:

If $|\mathrm{FSRI}^{(j)}| \geqslant \varepsilon_{h2,threshold}$ and $\mathrm{FSRI}^{(j)} > 0$,
Then, $\mathrm{FSRI}^{(j)} - \varepsilon_{h2,threshold} = F_h$;
If $|\mathrm{FSRI}^{(j)}| \geqslant \varepsilon_{h2,threshold}$ and $\mathrm{FSRI}^{(j)} < 0$,
Then, $\varepsilon_{h2,threshold} + \mathrm{FSRI}^{(j)} = F_h$.

In this paper, we select using fuzzy set of F_h to draw up the control command. That is to say, we map F_h value into several fuzzy sets, and corresponding to every fuzzy set, we design a kind of logical coordinated switching control commands. Firstly let us set a fuzzy domain and select a triangular membership function, through a quantitative factor, F_h can be mapped into 8-tuple fuzzy set {NB, NM, NS, NZ, PZ, PS, PM, PB} according to the range of its value, then based every fuzzy set, the logical coordinated switching control commands is design as follows.

The coordinated switching control commands regarding frequency as follows.

No command, if $|\mathrm{FSRI}^{(j)}| < \varepsilon_{h2,threshold}$.
Command 1: In light of the current state of storage energy unit agent, switch storage energy unit to suitable subsequent mode so as to decrease a small quantity of electrical energy output, if F_h is PZ.
Command 2: In light of the current state of storage energy unit agent, switch storage energy unit to suitable subsequent mode so as to decrease a certain quantity of electrical energy output, if F_h is PS.
Command 3: In light of the current states of both storage energy and renewable source unit agents, switch them to suitable subsequent modes so as to decrease a large quantity of real power output, if F_h is PM.
Command 4: In light of the current states of both storage energy and renewable source unit agents, switch them to suitable subsequent modes so as to decrease real power output to minimum value, if F_h is PB.
Command 5: In light of the current state of storage energy unit agent, switch storage energy unit to suitable subsequent mode so as to increase a small quantity of electrical energy output, if F_h is NZ.
Command 6: In light of the current state of storage energy unit agent, switch storage energy unit to suitable subsequent mode so as to increase a certain quantity of electrical energy output, if F_h is NS;
Command 7: In light of the current states of both storage energy and renewable source unit agents, switch them to suitable subsequent modes so as to increase a large quantity of real power output, or part of load shedding, if F_h is NM.
Command 8: In light of the current states of both storage energy and renewable source unit agents, switch them to suitable subsequent modes so as to increase real power output to maximum value, or load shedding, if F_h is PM.

According to the VSRI, the coordinated switching control regarding voltage is similarly to be drafted.

5. The lower level continuous control unit agents

In lower level unit control agents, the design of the continuous control of respective unit is highly dependent on its dynamic characteristic, control goal and operating mode, which is very different issue.

The continuous control of traditional generator is called as Power System Stabilizer (PSS), which is ordinarily designed as a double closed-loop controller including both power and voltage regulators. Authors have paid a great deal of attention on this issue and several approaches have been proposed in the author's previous publications [24,25]. The continuous control strategies of distributed generation units are usually divided into two kinds: grid-following control and grid-forming control. The grid-following control is usually selected as the control strategies of the non-dispatchable resources, which mainly includes MPPT control for the renewable energy resource units, V–Q control for the dc resource units and P–Q control. The grid-forming control is generally employed as the control strategies of the dispatchable resources, which mainly includes f–V control and load sharing based on droop characteristics. A dispatchable source is defined as a fast-response energy source which has adequate reserve capacity to meet the real and reactive transient-state power balance. Such a source may include interface through a power converter and storage devices on its DG side, such as a variable-speed wind-turbine based power generation unit connected through a back to back converter to micro-grid, or a fuel-cell powered converter. A non-dispatchable source is defined as a slow-response source which acts as an

uncontrollable source. The output powers of such a source are highly dependent on the pre-specified reference set values and/or the power provided by its prime source. The non-dispatchable sources contribute to supply the load demand based on the steady-state power balance and respond to small-signal disturbances. An example for is a photovoltaic source or a fix-speed wind-turbine based power generation source that relies only on solar radiations or wind resources with unpredicted, time-varying nature energy.

Typical f–V and P–Q controls are designed as shown in Figs. 6 and 7 respectively.

Because the local continuous need be frequently switched following the operation mode change, so beside the control scheme need be designed for distributed generation units, another important issue is how to select appropriate controller design algorithm to deal with robust stabilization problem at multi-mode switching scenarios. Since the multiple Lyapunov H_∞ stability method is considered as one of the best solution to deal with the multi-mode stability problem, therefore, in this section, the local continuous controller will be designed by using the state-feedback control based on the multiple Lyapunov H_∞ stability method, and detailed design is given as follows.

A general differential model of the controlled units is given as follows

$$\begin{cases} \dot{\boldsymbol{x}}_i(t) = (\boldsymbol{A}_{is} + \Delta\boldsymbol{A}_{is})\boldsymbol{x}_i(t) + (\boldsymbol{B}_{is} + \Delta\boldsymbol{B}_{is})\boldsymbol{u}_{is}(t) \\ \qquad\quad +(\boldsymbol{D}_{is} + \Delta\boldsymbol{D}_{is})\boldsymbol{\omega}_i(t), \\ \boldsymbol{z}_i(t) = \boldsymbol{C}_{is}\boldsymbol{x}_i(t), \quad i \in 1,2,\ldots N, \end{cases} \tag{22}$$

where $\boldsymbol{x}_i$ is the continuous state vector of the ith controlled unit; $\boldsymbol{u}_{is}$ is the state feedback control input of the sth operation mode in the ith controlled unit; $\boldsymbol{z}_i$ and $\boldsymbol{\omega}_i$ are the output and the disturbance of the ith controlled unit respectively; $\boldsymbol{A}_{is}$, $\boldsymbol{B}_{is}$, $\boldsymbol{C}_{is}$ and $\boldsymbol{D}_{is}$ are the coefficient matrices, and $\Delta\boldsymbol{A}_{is}$, $\Delta\boldsymbol{B}_{is}$ and $\Delta\boldsymbol{D}_{is}$ are uncertainty matrices.

The uncertainties in (22), which may be caused by various factors like disturbance at the switching instant, are assumed as norm-bounded in the following form

$$[\Delta\boldsymbol{A}_{is}\ \Delta\boldsymbol{B}_{is}\ \Delta\boldsymbol{D}_{is}] = \boldsymbol{H}_{is}\boldsymbol{F}_{is}(t)[\boldsymbol{E}_{1is}\ \boldsymbol{E}_{2is}\ \boldsymbol{E}_{3is}], \tag{23}$$

where $\boldsymbol{H}_{is}$, $\boldsymbol{E}_{1is}$, $\boldsymbol{E}_{2is}$ and $\boldsymbol{E}_{3is}$ are the real constant known matrices, and $\boldsymbol{F}_{is}(t)$ is an unknown matrix function with Lebesgue-measurable elements that satisfies $\boldsymbol{F}_{is}^T(t)\boldsymbol{F}_{is}(t) \leqslant \boldsymbol{I}^i$, in which $\boldsymbol{I}_i$ is the identity matrix.

The local state feedback control of the sth operation mode in the ith controlled unit is designed as

$$\boldsymbol{u}_{is}(t) = \boldsymbol{k}_{is}\boldsymbol{x}_i(t), \tag{24}$$

where $\boldsymbol{k}_{is}$ is the controller parameter in the sth operation mode of the ith controlled unit.

In addition, at the switching instant, the impulsive control is designed as

$$\Delta\boldsymbol{x}_i(t) = \Lambda_{is}\boldsymbol{x}_i(t), \quad t = t_s, \tag{25}$$

where t_s is the switching instant when the ith controlled unit is switched into the sth control mode from the $(s-1)$th control mode; $\Delta\boldsymbol{x}_i(t)$ is the impulsive vector of the continuous state and Λ_{is} is impulsive control parameter at the switching instant t_s.

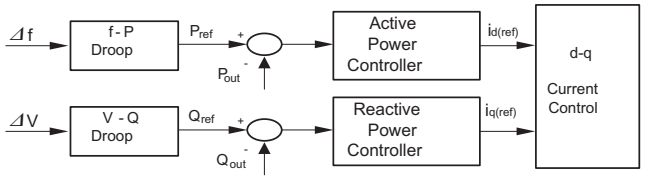

Fig. 6. f–V control strategy.

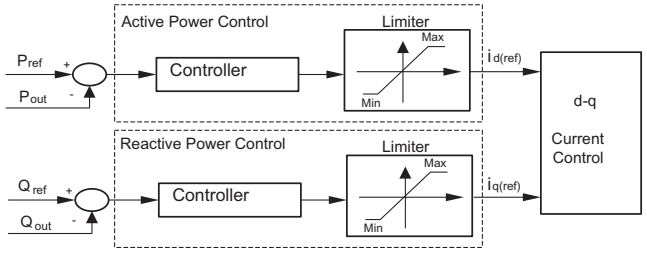

Fig. 7. P–Q control strategy.

Based on both state feedback and impulsive controls, the dynamic model can be rearranged in the following form

$$\begin{aligned} &\dot{\boldsymbol{x}}_i(t) = [\overline{A}_{is} + \boldsymbol{H}_i\boldsymbol{F}_{is}(t)(\boldsymbol{E}_{1is} + \boldsymbol{E}_{2is}\boldsymbol{k}_{is})]\boldsymbol{x}_i(t) + (\boldsymbol{D}_{is} + \Delta\boldsymbol{D}_{is})\boldsymbol{\omega}_i(t), \\ &\boldsymbol{z}_i(t) = \boldsymbol{C}_{is}\boldsymbol{x}_i(t), \\ &\Delta\boldsymbol{x}_i(t) = \Lambda_{is}\boldsymbol{x}_i(t), \quad t = t_s, \end{aligned} \tag{26}$$

where $\overline{\boldsymbol{A}}_{is} = \boldsymbol{A}_{is} + \boldsymbol{B}_{is}\boldsymbol{k}_{is}$;

$$\Delta\overline{\boldsymbol{A}}_{is} = \Delta\boldsymbol{A}_{is} + \Delta\boldsymbol{B}_{is}\boldsymbol{k}_{is} = \boldsymbol{H}_{is}\boldsymbol{F}_{is}(t)[\boldsymbol{E}_{1is} + \boldsymbol{E}_{2is}\boldsymbol{k}_{is}].$$

The multiple Lyapunov function of the ith closed-loop controlled unit in sth mode is defined as

$$V_{is}(t) = \boldsymbol{x}_i^T(t)\boldsymbol{P}_{is}\boldsymbol{x}_i(t), \tag{27}$$

where $\boldsymbol{P}_{is}$ is a symmetric positive weighting matrix.

Considering the initial condition, H_∞ performance related to the controlled output takes the form as

$$\int_0^{t_f} \boldsymbol{z}_i^T(t)\boldsymbol{z}_i(t)\mathrm{d}t \leqslant \rho_{is}^2 \int_0^{t_f} \boldsymbol{\omega}_i^T(t)\boldsymbol{\omega}_i(t)\mathrm{d}t + V_{is}(0), \tag{28}$$

where ρ_{is} is a prescribed attenuation level.

Theorem 1. *The controlled unit (26) can guarantee multi-mode robust stability by means of the state feedback control (24) integrated with the impulsive control (25), only if* $P_{is} = P_{is}{}^T > 0$, $P_{is-1} = P_{is-1}{}^T > 0$, $P_{is-1} = P_{is-1}{}^T > 0$, $\varepsilon_{is1} > 0$ *and* $\varepsilon_{is2} > 0$ *exist and are the common solutions of the following symmetric matrix inequalities,*

$$\begin{bmatrix} \boldsymbol{\Xi}_{11} & \boldsymbol{D}_{is} & \varepsilon_{is1}\boldsymbol{P}_{is}^{-1}(\boldsymbol{E}_{1is} + \boldsymbol{E}_{2is}\boldsymbol{k}_{is})^T & \boldsymbol{P}_{is}^{-1}\boldsymbol{C}_{is}^T \\ * & -\rho_{is}^2 + \varepsilon_{is2}\boldsymbol{E}_{3is}^T\boldsymbol{E}_{3is} & 0 & 0 \\ * & * & -\varepsilon_{is1}\boldsymbol{I} & 0 \\ * & * & * & -\boldsymbol{I} \end{bmatrix} \leqslant 0, \tag{29}$$

$$\begin{bmatrix} \boldsymbol{P}_{i(s-1)} & (\boldsymbol{I} + \Lambda_{is})^T\boldsymbol{P}_{is} \\ * & \boldsymbol{P}_{is} \end{bmatrix} > 0, \tag{30}$$

where $\boldsymbol{\Xi}_{11} = \overline{\boldsymbol{A}}_{is}\boldsymbol{P}_{is}^{-1} + \boldsymbol{P}_{is}^{-1}\overline{\boldsymbol{A}}_{is}^T + (\varepsilon_{is1}^{-1} + \varepsilon_{is2}^{-1})\boldsymbol{H}_{is}\boldsymbol{H}_{iz}^T$.

Proof. The derivative of $V_{is}(t)$ along the trajectory of system (26) satisfies

$$\begin{aligned} \dot{V}_{is}(t) = {} & 2\boldsymbol{x}_i^T(t)\boldsymbol{P}_{is}[\overline{\boldsymbol{A}}_{is} + \boldsymbol{H}_{is}\boldsymbol{F}_{is}(t)(\boldsymbol{E}_{1is} + \boldsymbol{E}_{2is}\boldsymbol{k}_{is})] + 2\boldsymbol{x}_i^T(t)\boldsymbol{P}_{is}(\boldsymbol{D}_{is} \\ & + \boldsymbol{H}_{is}\boldsymbol{F}_{is}(t)\boldsymbol{E}_{3is})\boldsymbol{\omega}_i(t). \end{aligned}$$

It is easy to obtain

$$\begin{aligned} \int_0^{t_f} \boldsymbol{z}_i^T\boldsymbol{z}_i\,\mathrm{d}t &= V_{is}(0) - V_{is}(t_f) + \int_0^{t_f} \left[\boldsymbol{z}_i^T\boldsymbol{z}_i + \dot{V}_{is}(t)\right]\mathrm{d}t \\ &\leqslant V_{is}(0) + \int_0^{t_f} \left\{ \begin{bmatrix} \boldsymbol{x}_i^T(t) & \boldsymbol{\omega}_i^T(t) \end{bmatrix} \begin{bmatrix} \boldsymbol{\Phi}_{11} & \Phi_{12} \\ \boldsymbol{\Phi}_{12}^T & -\rho_{is}^2\boldsymbol{I} \end{bmatrix} \right. \\ &\quad \left. \times \begin{bmatrix} \boldsymbol{x}_i^T(t) & \boldsymbol{\omega}_i^T(t) \end{bmatrix}^T + \rho_{is}^2\boldsymbol{\omega}_i^T(t)\boldsymbol{\omega}_i(t) \right\} dt. \end{aligned}$$

By observing the above result, it is obvious that the system of (26) has robust stability, if the following matrix inequality is satisfied, except at the switching instant,

$$\begin{bmatrix} \boldsymbol{\Phi}_{11} & \boldsymbol{\Phi}_{12} \\ \boldsymbol{\Phi}_{12}^T & -\rho_{\mathrm{is}}^2 \boldsymbol{I} \end{bmatrix} \leqslant 0, \tag{31}$$

where

$$\boldsymbol{\Phi}_{11} = \boldsymbol{P}_{\mathrm{is}}[\overline{A}_{\mathrm{is}} + \boldsymbol{H}_{\mathrm{is}}\boldsymbol{F}_{\mathrm{is}}(\mathrm{t})(\boldsymbol{E}_{1is} + \boldsymbol{E}_{2is}\boldsymbol{k}_{\mathrm{is}})] + [\overline{\boldsymbol{A}}_{\mathrm{is}} + \boldsymbol{H}_{\mathrm{is}}\boldsymbol{F}_{\mathrm{is}}(\mathrm{t})(\boldsymbol{E}_{1\mathrm{is}} + \boldsymbol{E}_{2\mathrm{is}}\boldsymbol{k}_{\mathrm{is}})]^T\boldsymbol{P}_{\mathrm{is}} + \boldsymbol{C}_{\mathrm{is}}^T\boldsymbol{C}_{\mathrm{is}};$$

$$\boldsymbol{\Phi}_{12} = \boldsymbol{P}_{\mathrm{is}}(\boldsymbol{D}_{\mathrm{is}} + \boldsymbol{H}_{\mathrm{is}}\boldsymbol{F}_{\mathrm{is}}(t)\boldsymbol{E}_{3\mathrm{is}}).$$

By using the Schur complement, then left and right multiplying matrix diag{$\boldsymbol{p}_{\mathrm{is}}{}^{-1}$, $\boldsymbol{I}$, $\boldsymbol{I}$, $\boldsymbol{I}$, $\boldsymbol{I}$}, the inequality (31) is equivalent to the inequality (29).

Table 5
Description of the connection situation of non-sensitive loads.

Simulation time (h)	Load 1	Load 2
0–2	X	
2–4	X	X
4–6		
6–8	X	X
8–10		X

X denotes loads connected, blank means loads disconnected.

Based on multi-mode stability theory, to ensure the system stability at the switching point, the following condition must be satisfied

$$\begin{aligned} V_i(t_s^+) - V(t_s^-) &= \boldsymbol{x}_i(t_s^+)^T\boldsymbol{P}_{\mathrm{is}}\boldsymbol{x}_i(t_s^+) - \boldsymbol{x}_i(t_s^-)^T\boldsymbol{P}_{i(s-1)}\boldsymbol{x}_i(t_s^-) \\ &= \boldsymbol{x}_i(t_s^-)^T[(\boldsymbol{I} + \boldsymbol{\Lambda}_{\mathrm{is}})^T\boldsymbol{P}_{\mathrm{is}}(\boldsymbol{I} + \boldsymbol{\Lambda}_{\mathrm{is}}) - \boldsymbol{P}_{i(s-1)}]\boldsymbol{x}_i(t_s^-) < 0. \end{aligned} \tag{32}$$

The above inequality is equivalent to inequality (30). This completes the proof. □

Denote $\tilde{\boldsymbol{k}}_{\mathrm{is}} = \boldsymbol{k}_{\mathrm{is}}\boldsymbol{P}_{\mathrm{is}}^{-1}, \overline{\boldsymbol{A}}_{\mathrm{is}}\boldsymbol{P}_{\mathrm{is}}^{-1} = \boldsymbol{A}_{\mathrm{is}}\boldsymbol{P}_{\mathrm{is}}^{-1} + \boldsymbol{B}_{\mathrm{is}}\tilde{\boldsymbol{k}}_{\mathrm{is}}$, and $\boldsymbol{P}_{\mathrm{is}}^{-1}(\boldsymbol{E}_{1\mathrm{is}} + \boldsymbol{E}_{2\mathrm{is}}\boldsymbol{k}_{\mathrm{is}})^T = \boldsymbol{P}_{\mathrm{is}}^{-1}\boldsymbol{E}_{1\mathrm{is}}^T + \tilde{\boldsymbol{k}}_{\mathrm{is}}^T\boldsymbol{E}_{2\mathrm{is}}^T$.

Then, the inequality (29) is a Linear Matrix Inequality (LMI).

In order to obtain a better robust performance, the H_∞ control performance can be treated as the following minimization problem, so that the H_∞ performance in (28) is reduced as much as possible

$$\begin{aligned} &\min \quad \rho_{\mathrm{is}}, \\ &\text{s.t.} \quad \text{the inequalities (29)and(30).} \end{aligned} \tag{33}$$

The minimization problem in (33) can be transformed into an LMI convex optimization problem. By using MATLAB toolboxes of LMI, the minimization H_∞ robust performance can be achieved, and the local state feedback control parameters and the impulsive control parameters can be obtained.

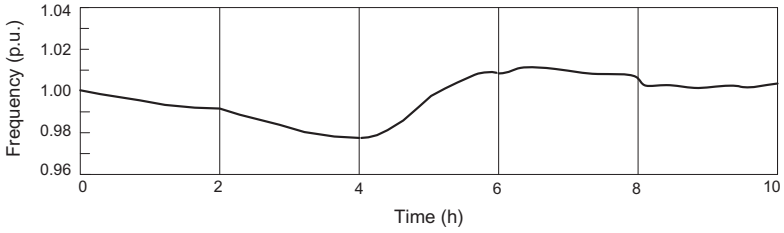

(a) The frequency performance in the case 1

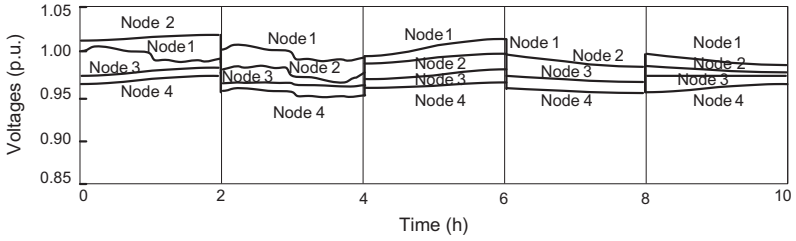

(b) The voltageperformancein the case 1

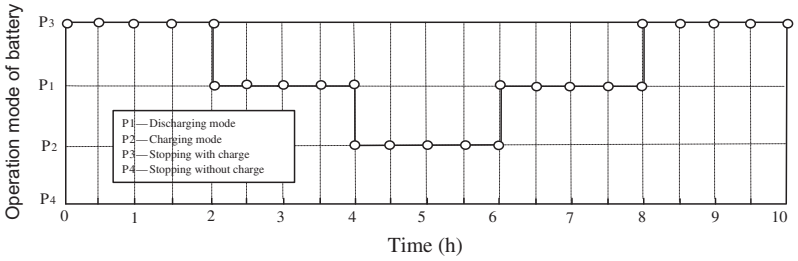

(c) The operating mode of the battery unit

Fig. 8. Load following performance in the case 1.

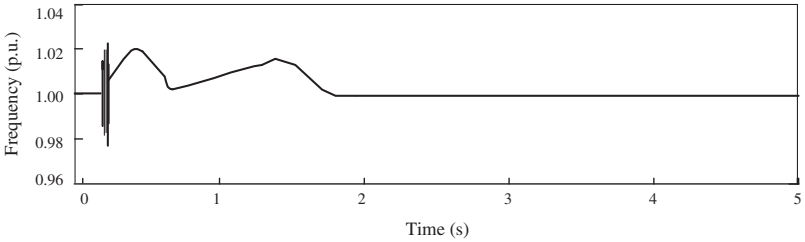

(a) The frequency performance in the case 2

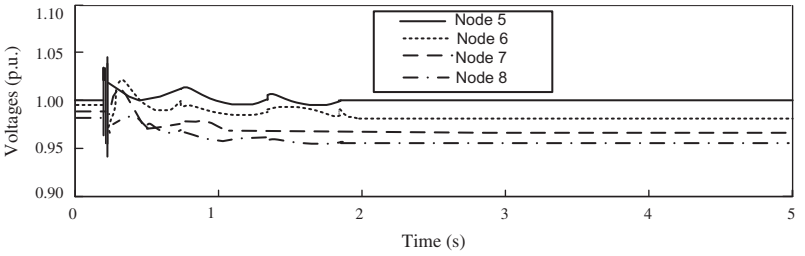

(b) The voltageperformance in the case 2

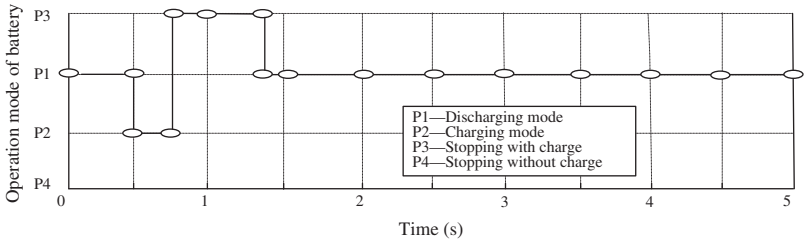

(c) The operating mode of the battery unit

Fig. 9. The performance after a transient disturbance in the case 2.

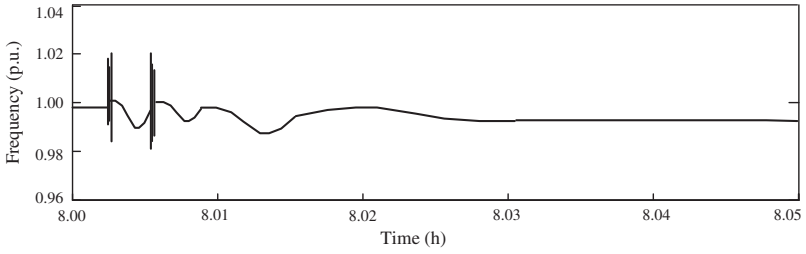

(a) The frequency in the case 3

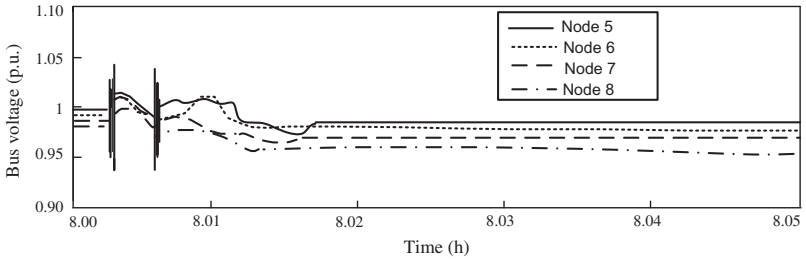

(b) The voltagesin the case 3

Fig. 10. The performance following an unplanned islanding in the case 3.

6. Simulation example

In this simulation study, a modified particle swarm optimization algorithm [20] is used to handle the energy management problem of the upper level agent. The continuous controller of the unit agent is design by using H_∞ robust stabilization method integrated with Linear Matrix Inequality (LMI) techniques, then using convex optimization technique of LMI in MATLAB toolbox,

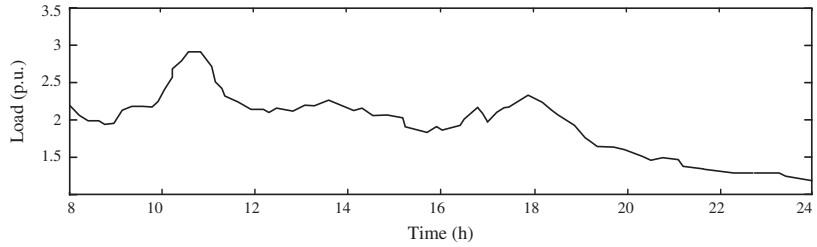

(a) Load curve of the islanded system in the region#2

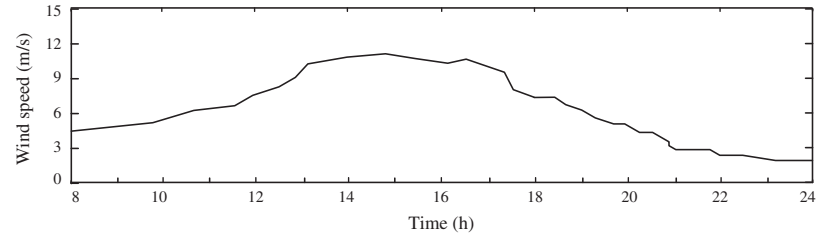

(b) Wind speed of the WT unit

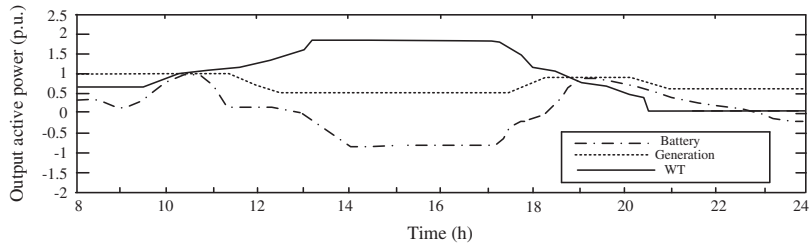

(c) Active powers of three generation units

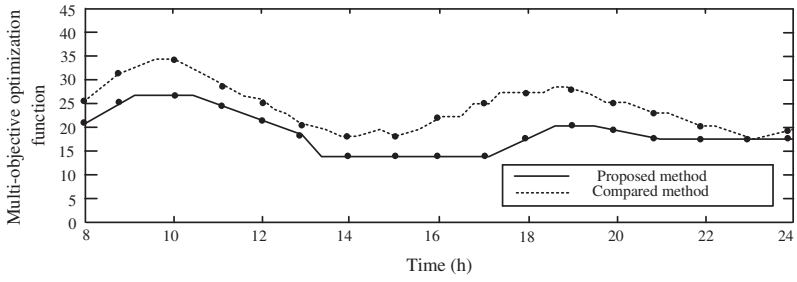

(d) Optimization performance of the islanded system

Fig. 11. Energy management optimization performance.

the multi-mode continuous controller parameters are obtained. The interactive behaviors among the different level of agents are implemented based on Foundation for Intelligent Physical Agents, Agent Communication Language (FIPA-ACL) in Java Agent Development Framework (JADF). FIPA-ACL messages are characterized by performative, conversation ID, content and receivers [26].

The case 1: Load following performance in regions#1.

In the case 1, the region #1 is taken as an example to test the control performance of voltages and frequency under load frequent change. And the connection situation of the non-sensitive loads in the region #1 is given in Table 5.

Following the change of loads, the performance of frequency and voltages are shown in Fig. 8. From Fig. 8(a), it can be observed that during most of the time, the frequency is below 1 p.u. but it is controlled between 0.98 p.u. and 1.02 p.u. During all of the simulation time, the fluctuation of frequency is limited in the range of ±2% of the nominal value. Fig. 8(b) shows the voltages of nodes 1, 2, 3 and 4. It can be seen that all voltage levels do not sink below 5% of nominal value during all of the simulation time, even if in bottom node 4. In this case, following the change of loads, only the operating mode of the battery unit is frequently switched to satisfy the variable load demand as shown in Fig. 8(c). The renewable energy unit always runs in MPPT mode without switching so as to guarantee the operating cost as small as possible. This case indicates that the MAS based hierarchical hybrid control is able to follow load change through switching the operating mode of the battery unit.

The case 2: Performance under a transient disturbance in region#2.

The purpose of this study is to investigate the performance of voltage and frequency after a transient large disturbance. This disturbance is designed as a short circuit fault that occurs on the

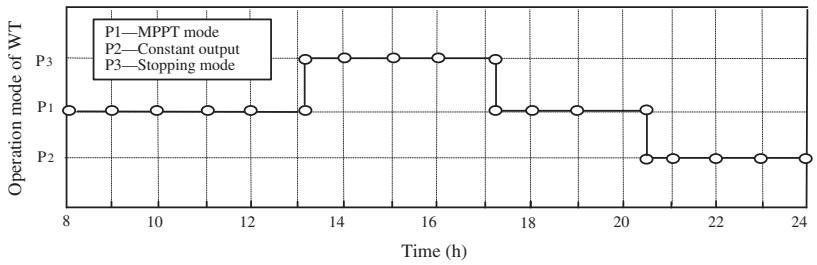

(a) Operating mode of the WT unit

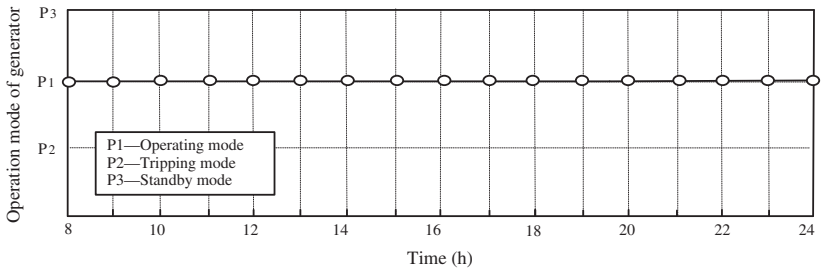

(b) Operating mode of the generator unit

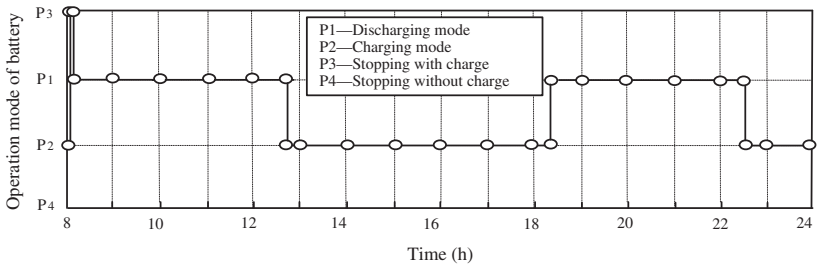

(c) Operating mode of the battery unit

Fig. 12. Operating modes of the three generation units in the case 3.

main-switch lines at $t = 0.2$ s and is cleared at $t = 0.3$ s so that the transmission lines are restored.

Fig. 9 shows the performance of voltage and frequency as well as the operation mode of the battery unit in the case 2. From Fig. 9, it is shown that only through three times switching of the battery unit at $t = 0.50$ s, 0.74 s, 1.35 s, respectively, the frequency rapidly settle down after $t = 0.85$ s, and frequency deviation is regulated less than ±2%. In addition, all voltages of nodes 5, 6, 7 and 8 in the region#2 are maintained within the range of security value during the disturbance, which are always not less than 95% of nominal value. It implies that the MAS based hierarchical hybrid control can maintain voltages and frequency in a secure level after a transient disturbance.

The case 3: Performance following permanent disturbance leading to an unplanned islanding in region#2.

The case 3 is firstly used to investigate self-healing performance regarding voltage and frequency after an unplanned islanding.

The unplanned islanding is caused by a permanent symmetrical three-phase short circuit fault that occurs on the line of main-switch at 8 am. And the fault sequence considered is in the following form:

Stage 1: The fault occurs at $t = 8.002$ h.
Stage2: The fault is removed by opening the main-switch of the faulted lines at $t = 8.0025$ h.
Stage3: The main-switch transmission lines are reconnected at $t = 8.005$ h. Since the fault is permanent, the reclosure is unsuccessful.
Stage 4: Islanding is formed in the region#2 by opening the main-switch of the faulted lines at $t = 8.0055$ h.

Fig. 10 shows the voltage and frequency performance during the islanding transient. From Fig. 10, it can be seen that in initial stage of islanding the voltage and frequency fluctuations are severe. After about 1.5 s, the voltages and frequency rapidly settle down. The reason is that in initial stage the operating mode of battery unit is frequently switched to maintain the balance between supply and demand. Just by switching the operating mode of the battery unit, during the islanding transient, the frequency variation of the islanded system is limited within 2% and the voltages of all nodes sink less than 5%. It implies that the proposed control scheme has the self-healing ability of the voltages and frequency after islanding transients.

In the following study, the simulation time is set form 8 h to 24 h for a typical summer day to test the energy management optimization performance of the islanded system. The load demand is shown in Fig. 11(a), and wind speed is shown in Fig. 11(b), which come from the real measurement data. By the means of the proposed control, three generation units (including generator unit, Wind Turbine (WT) unit and battery unit) supply active power for the load as shown in Fig. 11(c), and the optimization performance is shown in Fig. 11(d).

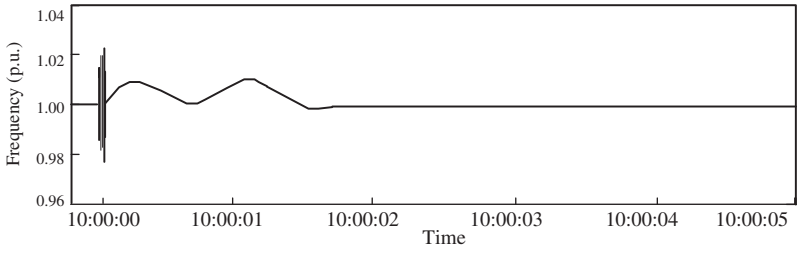

(a) The frequency performance in the case 4

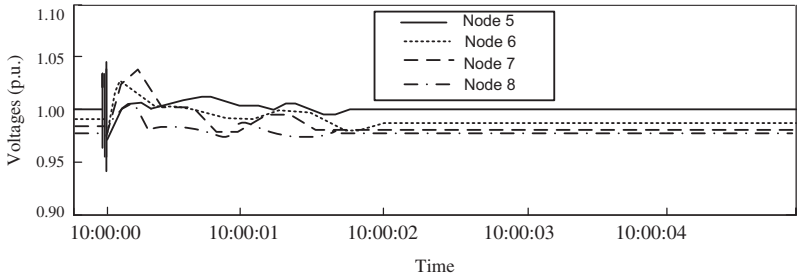

(b) The voltage performance in the case 4

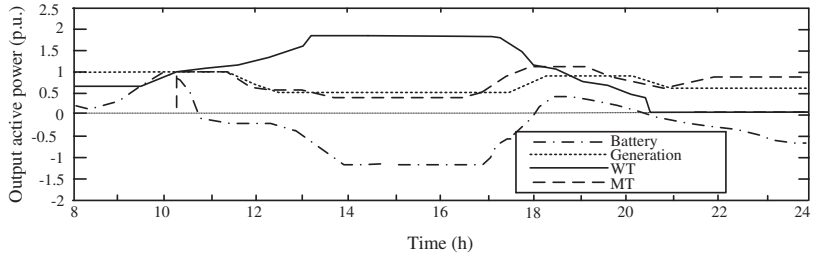

(c) The active powers of DERs

Fig. 13. The performance after a "plug-and-play" disturbance.

In this case, the operation modes of the three generation units are shown in Fig. 12.

From Figs. 11(c) and 12(a), it can be seen that WT unit runs in constant output mode form 13:10 pm to 17:15 pm because of the larger wind speed, and it stops operating after 20:30 pm due to the smaller wind speed, except the above time, the WT unit runs in MPPT mode according to the wind speed. During all of the simulation time, the operation mode of WT unit is switched three times, all of which are caused by wind speed. In addition, from Figs. 11(c) and 12(b), it can be observed that during all of the simulation time, the generator unit is always in the operating mode, but with a little change of output power that is regulated by its continuous controller. However, the operation mode of the battery unit is switched many times as shown in Figs. 11(c) and 12(c). Before 8:01 am, the battery unit is switched two times from charging mode to stopping mode, again from stopping mode to discharging mode. The reason is that in initial stage of islanding, the voltages and frequency of the islanded system are mainly maintained by the switching control for battery unit in order to maintain the balance between supply and demand. After 8:01 am, the operation mode of the battery unit is switched three times by the coordinated control agent. From the power assignments as shown in Fig. 11(c), it can be implied that the operating mode of the generator unit is not switched as far as possible because of its low efficiency during starting, and the renewable energy unit runs in MPPT mode as far as possible because of its free operating cost, only battery unit is responsible for maintaining the balance between supply and demand by the frequent switching of operating mode. It also indicates that the energy management strategies can obtain minimum cost performance. Finally, a comparison of optimization performance between the proposed method and the method in [20] is shown in Fig. 11(d). It can be observed that the proposed control can achieve smaller operation cost.

The case 4: Performance following "plug-and-play" of DERs in region#2.

The purpose of this study is to investigate the performance of scalability via "plug-and-play" of DER unit in region#2. This case is designed that a micro-turbine (MT) generation unit agent is connected into the region#2 nearby the node 8 at $t = 10$ h.

Fig. 13(a) and (b) shows the performance of voltage and frequency. It can be seen that frequency deviation is maintained in range of ±1% of rated value. In addition, all voltages of nodes 5, 6, 7 and 8 in the region#2 are not less than 97% of nominal value. It shows that the MAS based hierarchical hybrid control can rapidly adjust voltages and frequency to return into a normal level after plugging a DER unit agent. It also implies that the MAS based control can permit "plug-and-play" of DER and has better scalability performance. Fig. 13(c) shows active powers of all DERs in region#2, which supply for the load as shown in Fig. 11(a). From Fig. 13(c), it can be seen that the renewable energy resource WT unit always runs in MPPT mode without switching so as to guarantee the operating cost as small as possible, both MT and generator units operate in rated state so as to ensure high-efficiency, and only battery unit is frequently switched so as to maintain power

balance between supply and demand. It also indicates that the energy assignment among DERs can achieve cost performance optimization.

7. Conclusion

In this paper, a MAS based hierarchical hybrid control for high-penetrated distribution grids is presented for improving the integrative performance regarding dynamic stability, self-healing, security, as well as economic and environmental benefits. In the upper level agent, the energy management model and optimization objective function are constructed in order to design and implement the optimization management strategies. Moreover, in the middle level agents, in order to implement the coordinated switching control of operating mode, the operating mode cooperation control model and the coordinated switching control strategies are designed respectively. All of above are innovative works. Simulation results have shown that following load changes and under significant disturbances, the MAS based hierarchical hybrid control can maintain better performance regarding security and stability as well as minimum operating cost by real-time switching of operational mode.

The MAS based hierarchical control is one of the best choices to make much smart grid. It provides a feasible solution to use combination of artificial intelligence and mathematical tools to decide hybrid control actions. The MAS based hierarchical control can be easily extendable for managing and controlling any kind of power system with distributed resource by extending the function of the agents and creating additional agents in the system.

Acknowledgments

This work is supported by the National Natural Science Foundation of China Nos. 51177142 and 61174075, and is also supported by Hebei Provincial Natural Science Foundation of China No. F2012203063 and Hunan Provincial Natural Science Foundation of China No. 11JJ2038.

Appendix A. Supplementary material

Supplementary data associated with this article can be found, in the online version, at http://dx.doi.org/10.1016/j.ijepes.2013.07.029.

References

[1] Wang W, Bai X, Zhao W, Ding J, Fang Z. Hybrid power system model and the method for fault diagnosis. In: IEEE/PES transmission and distribution conference and exhibition. Asia and Pacific, Dalian, China; 2005.
[2] Gao L, Jiang Z, Dougal RA. An actively controlled fuel cell/battery hybrid to meet pulsed power demands. J Power Sour 2004;130:202–7.
[3] Jeong KS, Lee WY, Kim CS. Energy management strategies of a fuel/battery hybrid system using fuzzy logics. J Power Sour 2005;145:319–26.
[4] El-Shater FT, Eskander NM, El-Hayry TM. Energy flow and management of a hybrid wind/PV/fuel cell generation system. Int J Sustain Energy 2006;25:91–106.
[5] El-Shater FT, Eskander NM, El-Hayry TM. Energy flow and management of a hybrid wind/PV/fuel cell generation system. Energy Convers Manage 2006;47:1260–80.
[6] Hi H, Heydt GT, Mill L. Power system stability agents using robust wide area control. IEEE Trans Power Syst 2002;17:1123–31.
[7] Kamwa I, Grondin R, Hebert Y. Wide-area measurement stabilizing control of large power systems – a decentralized/hierarchical approach. IEEE Trans Power Syst 2001;16:136–53.
[8] Mcarthur SDJ, Davidson EM, Catterson VM, et al. Multiagent systems for power engineering applications, Part I: Concepts, approaches, and technical challenges. IEEE Trans Power Syst 2007;22:1743–52.
[9] Mcarthur SDJ, Davidson EM, Catterson VM, et al. Multiagent systems for power engineering applications, Part II: Technologies, standards, and tools for building multiagent systems. IEEE Trans Power Syst 2007;22:1753–9.
[10] Liu CC. Agent modeling for integrated power systems. Final Project Report, Power Systems Engineering Research Center, PSERC Publication 08–17, September; 2008.
[11] Dimeas AL, Hatziargyrious ND. Agent based control for Microgrids. In: IEEE PES general meeting, Tampa, FL; June 2007. p. 24–28.
[12] Hill DJ, Gao Y, Larsson M. Global hybrid control of power systems. Preprints of bulk power system dynamics and control V, vol. 8; Japan 2001. p. 26–31.
[13] Leung JSK, Hill DJ, Ni YX. Global power system control using generator excitation, PSS, FACTS, devices and capacitor switching. Int J Electr Power Energy Syst 2005;27:448–64.
[14] Zhao HS, Mi ZQ, Niu DX, et al. Power system modeling using hybrid system theory. Proc CSEE 2005;23:20–5 [in Chinese].
[15] Zhao HS, Mi ZQ, Song W, et al. Model and switching stability analysis of hybrid power system with OLTC. Autom Electr Power Syst 2003;273:24–8 [in Chinese].
[16] Donde V. A hybrid system using two cascaded regulators. ECE Dep.; 2000.
[17] Dou CX, Mao CC, Zhang XZ, Guan XP. Hybrid control for wide-area power systems based on hybrid system theory. Int J Syst Sci 2011;42:201–17.
[18] Dou CX, Liu B. Hierarchical hybrid control for improving comprehensive performance in smart power system. Int J Electr Power Energy Syst 2012;43:595–606.
[19] Park JH, Rovoliotis S, Bodner D, Zhou C, Meginnis L. A colored Petri net-based approach to the design of 300 mm wafer fab controller. In: Proceedings of the 2001 IEEE international on robotics & automation. Korea; 2001.
[20] Dou CX, Jia XB, Bo ZQ, Zhao F, Liu DL. Optimal management of microgrid based on a modified particle swarm optimization algorithm. In: Asia-Pacific power and energy engineering conference. Wuhan, China; 2011.
[21] Ye YD, Zhang L, Jia LM. Research on agent-based G-Net train group operation model. In: Fifth world congress on intelligent control and automation; 2004.
[22] Anderson PM, Mirheydar M. An adaptive method for setting under frequency load shedding relays. IEEE Trans Power Syst 1992;7:647–55.
[23] Seethalekshmi K, Singh SN, Srivastava SC. A synchrophasor assisted frequency and voltage stability based load shedding scheme for self-healing of power system. IEEE Trans Smart Grid 2011;2:221–30.
[24] Dou CX, Zhang XZ, Guo SL, Mao CC. Delay-independent excitation control for uncertain large power systems using wide area measurement signals. Int J Electr Power Energy Syst 2010;32:210–7.
[25] Dou CX, Duan ZS, Jia XB. Delay-dependent H_∞ robust control for large power systems based on two-level hierarchical decentralized coordinated control structure. Int J Syst Sci 2012;43:1–17.
[26] Dou CX, Liu B. Multi-agent based hierarchical hybrid control for smart Microgrid. IEEE Trans Smart Grid 2013;4:771–8.